Cross-Field Resistivity Scaling With Density and Temperature For Steady State FRCs Under Rotating Magnetic Field Current Drive

A.L. Hoffman, H.Y. Guo, K.E. Miller, R.D. Milroy

Redmond Plasma Physics Laboratory, University of Washington, Seattle, WA, USA

e-mail contact of main author: hoffman@aa.washington.edu

Abstract: FRCs can be sustained in steady state by Rotating Magnetic Fields (RMF) at densities relevant to fusion reactors. The obtainable density scales linearly with the RMF magnitude B_ω and inversely with the plasma resistivity. The RMF power required to sustain the FRC current and flux is also directly proportional to the square of the total toroidal current and the average resistivity. It has been found in TCS (Translation, Confinement, Sustainment) experiments that as the plasma temperature is increased by using anti-symmetric RMF drive, or by reducing the impurity level, that despite higher currents and magnetic fields, the RMF power required to maintain the configuration does not increase significantly. This is due to most of the added diamagnetic current being carried in a low resistivity core near the FRC field null, and also to a resistivity that appears to scale as B^{-1}. Past experiments have been limited in temperature by high impurity levels and low Z radiation barriers, and experiments at higher temperatures will soon be underway in a new device, TCS/upgrade, significantly upgraded to produce clean plasmas.

1. Introduction

FRCs have the highly desirable and unique fusion confinement features of very high beta, a natural unconstrained divertor, and simple singly-connected cylindrical geometry. The recent adaptation of Rotating Magnetic Field (RMF) current drive pioneered in Australian rotamak experiments [1] has provided a means of creating and sustaining FRCs in the relatively new TCS (Translation, Confinement, Sustainment) FRC facility [2]. FRCs have been formed and maintained in quasi steady-state (governed only by power supply pulse length) in the reactor relevant density regime of 10^{19}–10^{20} m^{-3} [3]. RMF reverses the normal outward plasma diffusion and provides long particle confinement times, so the principal reactor concerns are energy confinement, power balance, and stability. When a RMF of magnitude B_ω partially penetrates the FRC it produces a strong inward radial pressure $\sim B_\omega^2/\mu_o$ which is strongly stabilizing against interchange modes [4]. This partial penetration, when combined with an anti-symmetric antenna arrangement, results in completely closed field lines, and has been measured to reduce all losses other than radiation to low levels [5]. An FRC is a diamagnetic entity, so that toroidal currents are present simply due to the FRC pressure. Steady-state sustainment then becomes a matter of the RMF power needed to maintain $E_\theta(r) = 0$ in the face of plasma resistivity, and maintain the FRC poloidal flux. (For an elongated FRC a simple 2-D analysis considers θ as the toroidal/azimuthal direction and z as the poloidal direction.)

RMF current drive works by exerting an azimuthal force on the plasma electrons in the direction of the RMF rotation. The penetration of the RMF into a plasma column is given by $\delta^* = (2\eta/\mu_o\varpi)^{1/2}$ where η is the plasma resistivity and $\varpi = \omega - \omega_e$ is the difference between the RMF frequency and the electron rotation rate. The resistivity is relatively high near the FRC separatrix r_s, and the RMF drives the outer electrons into near synchronous rotation ($\varpi << \omega$), which results in typical RMF penetration distances of order $\delta^* \sim 0.2r_s$. This is nearly ideal from the point of view of maximizing torque, providing strong stabilization against interchange modes, and maintaining closed field lines (when using anti-symmetric RMF antennas). Equating the electron-ion frictional torque (resistivity) with the RMF torque

provides an accurate measure of the average plasma resistivity. In a diamagnetic entity, the cross-field resistivity is an indication of the over-all micro-turbulence level, which will affect all transport properties. Besides being a simple and attractive confinement scheme, the FRC also provides a unique and straightforward platform for studying such transport.

2. Analysis

Calling B_r and B_θ the radial and azimuthal components of the RMF in the plasma, the azimuthal force on the electrons is produced by an induced axial electron oscillation, v_{ez}, in phase with B_r, $F_\theta = -n_e e\langle v_{ez}B_r\rangle$. (The radial force is $F_r = -n_e e\langle v_{ez}B_\theta\rangle$.) The azimuthal electric field is given by $E_\theta = \eta_\perp j_\theta + \langle -v_{ez}B_r\rangle + v_{er}B_z$ and must be zero everywhere for the FRC flux to remain constant. For clockwise RMF rotation (B_z positive external to the FRC) j_θ is negative and reverses the external field. A positive $\langle -v_{ez}B_r\rangle$ can balance the negative resistive term, but if the RMF only partially penetrates the FRC an inward (negative) v_{er} is needed in the FRC interior where $B_z(r)$ is negative. Most analysis has assumed that in the outer regions (outside the field null at R where $B_z(R) = 0$) the RMF term is not only strong enough to balance the negative $\eta_\perp j_\theta$, but also results in an inward v_{er}. A swirling current or particle flow is assumed, returning at the FRC ends. In 2-D numerical calculations, this particle flow is forced by removing particles on the inner field lines, and inserting them on corresponding outer field lines, to maintain equal pressures on the same flux surface [6]. Resistive drag on the electrons occurs throughout the FRC, and a torque based model has been used to analyze the overall force balance [7].

The rate of FRC flux build-up can be described by

$$\frac{d\phi_p}{dt} = \frac{2}{n_e e r_s^2 \ell_s}\left(T_{RMF} - T_\eta\right) \qquad (1)$$

where $r_s = \sqrt{2}R$ is the FRC separatrix radius and ℓ_s is the separatrix length. The RMF torque is given by

$$T_{RMF} = T_o'\left(\frac{\delta^*}{r_s}\right)\ell_a \qquad T_o' = \frac{2\pi r_s^2 B_\omega^2}{\mu_o} \ . \qquad (2)$$

where ℓ_a is the RMF antenna length [7]. The frictional resistive torque is $T_\eta = \int_0^{r_s} 2\pi e^2 n_e^2 \omega_e \eta_\perp r^3 dr \ell_s$ where ω_e is the electron rotational speed (with the ions assumed stationary) and ℓ_s is the FRC separatrix length. Many properties of the RMF sustained FRC indicate that the resistivity profile, $\eta(r)$, is very non uniform [8]. Its density and magnetic field profiles are well described by a double rigid rotor model (DRR) with an electron rotation speed $\omega_e = \omega_r$ in the inner region near the field null, and $\omega_e = 2\omega_r$ for the outer region ($r > 0.87r_s$) [9]. A simplified approximation to a non uniform resistivity profile is to specify a resistivity η_i in the inner region, and η_e in the edge region. ($r < 0.5r_s$ is also considered the edge region, but has very little effect on the resistive torque.) The resistive torque can then be calculated as

$$T_\eta = 1.07\pi e n_m \left(\frac{B_e}{\mu_o}\right) r_s^2 \left(\eta_i + 0.29\eta_e\right)\ell_s \ , \qquad (3)$$

where n_m is the peak electron density and B_e the external magnetic field. The power absorbed due to the theta currents can also be calculated as $P_\theta = \int_0^{r_s} \eta_\perp j_\theta^2 2\pi r dr \ell_s$ where $j_\theta = -n_e e \omega_e r$.

This is identical to using the integral expression for torque with ω_e^2 inside the integral. Any ion rotation can be accounted for by multiplying the torque by the actual ω_e ($\omega_r + \omega_i$ in the center, and $2\omega_r + \omega_i$ at the edge). Then

$$P_\theta = \pi\left(\frac{B_e}{\mu_o}\right)^2 \left(4(1+\omega_i/\omega_r)\eta_i + 2.3(1+\omega_i/2\omega_r)\eta_e\right)\ell_s \ . \qquad (4)$$

In the above analysis, $B_e = 0.27\mu_o n_m e\omega_r r_s^2$.

3. Density & Power Absorption Measurements

The DRR description is more accurate in describing the FRC density and magnetic field profiles than that those used in a previous model [3], where the electrons were assumed to be rotating as a rigid rotor except in a very thin edge layer where they rotated synchronously with the RMF with $\omega_e = \omega$. $n_e(r)$ and $B_z(r)$ are plotted in Fig. 1 for a typical discharge at two times. The DRR profile is seen to be a fairly good match to the experimental profiles.

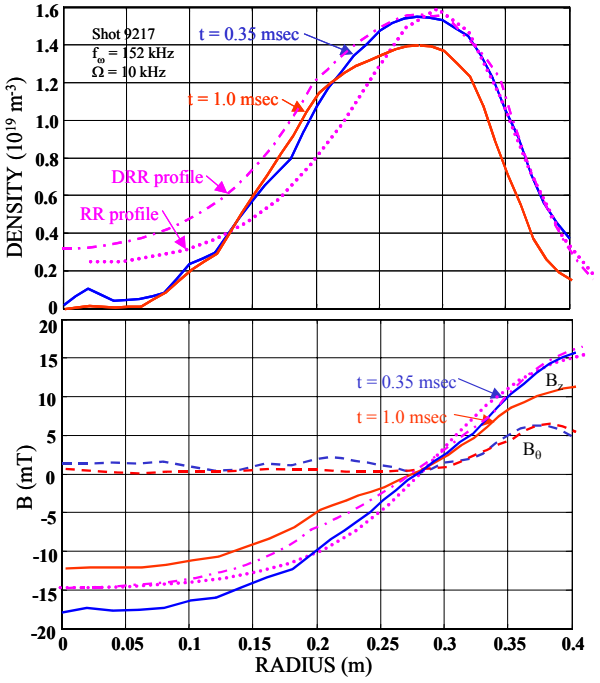

FIG 1. Density and magnetic field profiles at early and late times. The dotted lines are for a RR profile with K_{RR} = 1.5, and the dash-dotted lines represent the DRR profile.

Using the DRR model with a somewhat arbitrary assignment of $\eta_e = 10\eta_i$, and equating the torques given by Eqs. (2) and (3) with ℓ_a equal to ℓ_s as is approximately true for most experiments, the peak density scales as

$$n_{mDRR}(10^{19}\,m^{-3}) = 0.67\frac{B_\omega(\mathrm{mT})(\delta^*/r_s)^{1/2}}{\omega_r^{1/2}(10^6\,\mathrm{rad/s})\,r_s(\mathrm{m})\,\eta_i^{1/2}(\mu\Omega\text{–m})} \ . \qquad (5)$$

It might be expected that the ratio δ^*/r_s would increase with the ratio ω_r/ω, as has been assumed in some modeling, but this scaling is observed to be very weak, at least for ω_r/ω values under 0.2. This same weak scaling is also seen in numerical calculations when a very non-uniform resistivity profile is specified. In any case, the scaling of Eq. (5) can be used along with measured values of δ^* and ω_r to determine η_i. The peak density is plotted in Fig. 2 versus a factor representing the ratio of RMF to resistive torques. A best fit to the experimental data, ignoring the effect of temperature, is

$$n_{m\exp}(10^{19}\,\mathrm{m}^{-3}) = 0.096\frac{B_\omega(\mathrm{mT})(\delta^*/r_s)^{1/2}\,n_m^{1/4}(10^{19}\,\mathrm{m}^{-3})}{\omega_r^{1/2}(10^6\,\mathrm{rad/s})\,r_s(\mathrm{m})} \ . \qquad (6)$$

It is written in this form for direct comparison to Eq. (5), which yields

$$\eta_i = \frac{50}{n_m^{1/2}(10^{19}\,\mathrm{m}^{-3})}\ \mu\Omega\cdot\mathrm{m}\ . \qquad (7)$$

This is the same density dependence deduced from flux decay rates in high density θ-pinch formed FRCs [10].

Two numerical calculations are also shown in Fig. 2. They were performed with a specified resistivity profile of $\eta_\perp(r) = \eta_o + \eta_e/\{1 + \exp[(r_s\text{-}r)/\delta_e]\}$ with η_o = 31 μΩ-m, η_e = 1200 μΩ-m, and δ_e = 1 cm. This is a fairly extreme profile, but it is typical of what we would expect from previous empirical scaling based on an anomalous collision frequency strongly dependent on the ratio v_{de}/v_{ti} of electron drift velocity to ion thermal speed (or sometimes ion sound speed v_s). The electron drift velocity near the outer edge of an RMF driven FRC is close to ωr_s, while it drops to $\omega_r R$ near the field null, which can be a difference of almost an order of magnitude. In the numerical calculations some of the initially applied RMF gets trapped in the higher conductivity interior, and rotates with the electrons there. This has been called an 'edge driven mode' (edm). Clear indications are seen of this mode in most experiments [8]. Numerically, if the inner resistivity were assumed higher, the edm would decay away very quickly, and if the outer resistivity were made lower, an edm would never develop. It thus appears that the resistivity profile assumed for the numerical calculations is fairly representative of the true profile, and that the simple η_i, η_e analytical modeling is a crude approximation, which is nevertheless useful since other assumptions do not change the derived results very strongly. More details about the calculations are given in Ref. 9.

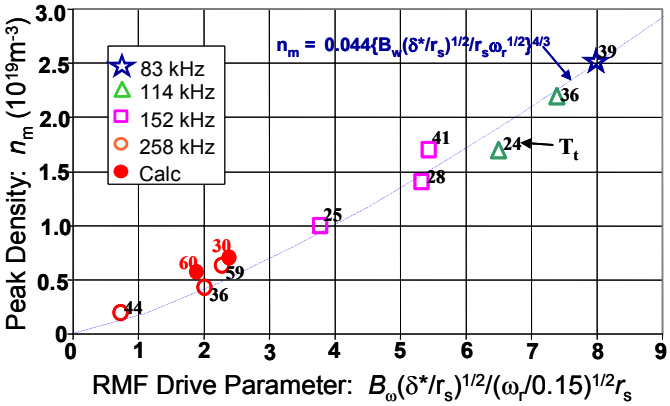

FIG 2. Measured peak FRC density versus scaling parameter. The RMF frequencies f_ω are listed, as are the total temperatures (in eV) for each data point.

The flux in the TCS FRCs was sustained by the RMF, but the particle inventory was sustained solely by recycling. TCS had no baking or wall conditioning, and used plastic sealing rings and greased elastomer O-rings. This resulted in very high impurity levels after the first half msec. Somewhat higher temperatures were achieved during the initial start-up, but were then quickly reduced as the impurity level rose. The temperature variations shown in the data of Fig. 2 was due to these varying conditions. It can be seen that better scaled results (n_m values above the scaling curve) were always obtained at the higher total temperature, T_t. This is in spite of the fact that the resistive torque scales as $T_\eta \propto \eta_\perp n_e^{3/2} T_t^{1/2} r_s^2$. Thus, the resistivity must be dropping with temperature, as would be expected when v_{de}/v_s decreases (mostly near the edge since $v_{de} = \omega_r r$, as well as v_s, increases with $T_t^{1/2}$). The numerical calculations made for the specified (unchanging) resistivity profile, but for two different temperatures, show the expected density reduction as the temperature increases. The experimental results thus indicate a resistivity dependence inversely proportional to temperature as well as density.

A practical measure of performance is the RMF power required to drive a given current. Based on Eq. (4) it is instructive to plot the ratio of absorbed power to $B_e^2 \ell_s$. This is done in Fig. 3 as a function of the square of the B_e/B_ω ratio for operation at various RMF frequencies. The normalization is based on $\eta_e = 10\eta_i$ and ω_i taken as zero. The vertical axis of the graph is not an actual resistivity, but if we call it ηabs, it can be used to calculate the power required to sustain an FRC contained in a external magnetic field of magnitude B_e.

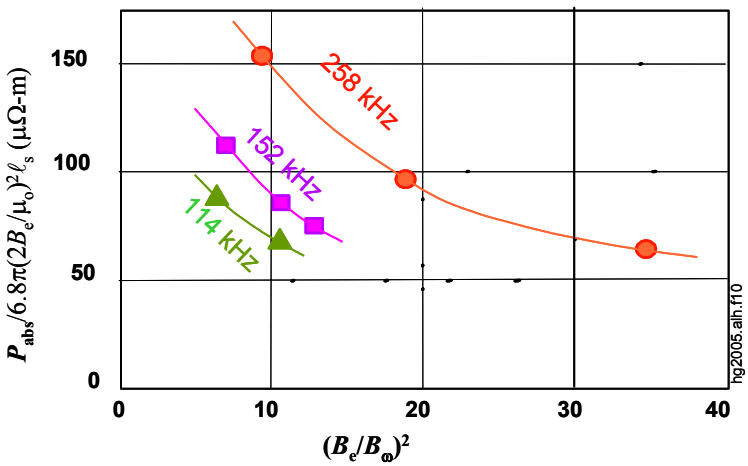

FIG 3. Relative absorbed power versus B_e/B_ω ratio.

$$P_{RMF} = \eta_{abs}\left[6.8\pi\left(\frac{2B_e}{\mu_o}\right)^2\right]\ell_s \qquad (8)$$

The different frequency operating conditions are lumped together since they represent different densities ($n_e \sim\propto f_\omega^{-1/2}$). The 'effective' resistivities of Fig. 3 are about twice as high as given by Eq. (7). This is due slightly to a larger contribution of the theta current in the edge region to power than to torque, but is mainly due to a large amount of power being dissipated by the j_z axial shielding currents which govern RMF penetration.

The power absorbed by the axial shielding currents is $P_z = \int_0^{r_s} \eta_{//} j_z^2 2\pi r dr \ell_s$. Within the confines of our simple model, with $\eta_{//}$ taken the same as $\eta_\perp$, this can be expressed as

$$P_z \approx 2\pi \frac{r_s}{\delta^*}\left(\frac{B_\omega}{\mu_o}\right)^2 \eta_e \ell_s \ . \qquad (9)$$

The total absorbed power is $P_{RMF} = P_\theta + P_z$. Thus, it is reasonable to plot the normalized absorbed power as a function of $(B_e/B_\omega)^2$. Since $n_m \propto B_\omega$ and $B_e \approx (2\mu_o n_m k T_t)^{1/2}$, $(B_e/B_\omega)^2 \propto T_t/n_m$. Higher values of B_e/B_ω are naturally obtained at higher temperatures, usually with very little additional required power. The reason TCS could achieve higher ratios of B_e/B_ω at the higher RMF frequency is that the total temperature tended to be limited by radiation barriers, and the ratio of T_t/n_e was higher at the lower densities.

The resistivity profile used in the calculations was chosen based on the empirical 'Chodura' formula, $\nu_{ch} \sim \omega_{pi}(1 - \exp[-v_{de}/v_s])$ with $\eta_{ch} = m_e \nu_{ch}/n_e e^2$, which has been used to model diffusion in pinches [11] and θ-pinch formation and decay of FRCs [12]. v_{de} is the electron drift speed, and v_s is the ion sound speed. Near the edge of the FRC $v_{de} \approx \omega r_s$, which is much larger than v_s, and the resistivity is very high. Recent 2-fluid calculations at the University of Washington support the above scaling, showing rapid non-linear turn-on of drift-wave turbulence when v_{de} approaches v_s. [13]. The TCS torque and power measurements provide a

means of inferring the resistivity profiles, and of bench-marking the more general two-fluid calculations.

It has also been noted in scaling from a smaller r_s = 20 cm diameter experiment that the resistivity is dropping with size, as expected from the Chodura formula, so that RMF current drive should scale favorably to future hotter and larger devices with smaller v_{de}/v_s. TCS is presently being extensively modified to provide mostly all metal construction in a bakable chamber, and it is expected that much higher T_t will be obtainable when used in conjunction with anti-symmetric RMF. This will allow us to test the resistivity temperature scaling over a much wider range.

References

[1] JONES, I.R., "*A review of RMF current drive and the operation of the rotamak as an FRC and an ST*", Phys. Plasmas **6**, 1950 (1999).

[2] HOFFMAN, A.L., et. al. "*The TCS Rotating Magnetic Field FRC current drive experiment*", Fusion Technology **41**, 92 (2002).

[3] HOFFMAN, A.L., GUO, H.Y., MILLER, K.E., MILROY, R.D., "*Long pulse FRC sustainment with enhanced edge driven RMF current drive*" Nucl. Fusion **45**, 176 (2005).

[4] GUO, H.Y., et.al., "*Stabilization of interchange modes by RMF current drive*" Phys. Rev. Lett. **94**, 185001 (2005).

[5] GUO, H.Y., HOFFMAN, A.L., STEINHAUER, L.C., "*Observations of improved confinement in FRCs sustained by anti-symmetric RMF*", Phys. Plasmas **11**, 1087 (2005).

[6] MILROY, R.D., "*A magnetohydrodynamic model of rotating magnetic field current drive in a field-reversed configuration*", Phys. Plasmas 7, 4135 (2000).

[7] HOFFMAN, A.L., "*Rotating magnetic field current drive of FRCs subject to equilibrium constraints*", Nuclear Fusion, 40, 1523 (2000).

[8] MILROY, R.D. K.E. MILLER, "*Edge-driven RMF current drive of FRCs*", Phys. Plasmas **11**, 633 (2004).

[9] HOFFMAN, A.L., et.al., "*Principal physics of RMF current drive of FRCs*", Phys. Plasmas **13**, 012507 (2006).

[10] HOFFMAN, A.L., Slough, J.T., "*FRC lifetime scaling based on LSX measurements*", Nucl. Fusion **33** 27 (1993).

[11] SGRO, A.G., NIELSON, C.W., "*Hybrid model studies of ion dynamics and magnetic field diffusion during pinch implosions*", Phys. Fluids **19**, 126 (1976).

[12] MILROY, R.D., SLOUGH, J.T., "*Poloidal flux loss & axial dynamics during the formation of FRCs*", Phys. Fluids **11**, 3566 (1987).

[13] LOVERICH, J., SHUMLAK, U., "*Non-linear 2-fluid study of instabilities in an axisymmetric Z-pinch*", to be published.